Copyright © 2003. Paper 7-005; 9034 Words, 8 Figures.
http://EarthInteractions.org

Positive Feedback and System Resilience from Graphical and Finite-Difference Models: The Amazon Ecosystem—An Example

J. Alcock*

Department of Environmental Sciences, The Pennsylvania State University, Abington College, Abington, Pennsylvania

Received 18 August 2002; accepted 16 December 2002

ABSTRACT: Positive feedback has the potential to create multiple steady states that divide system space into regions of distinct behavioral modes. Graphical analysis can be used to recognize systems likely to behave in this way. For example, positive feedback created by interactions among tropical forest, regional hydrology, and climate in the Amazon basin may produce multiple steady states. As deforestation progresses, one state—the normal forest with a high leaf area index—is stable and promotes system resilience. However, deforestation can cause the system to shift toward and past a second, unstable state at moderate levels of forest cover. The latter separates forest stability in the face of stress from runaway behavior and system collapse into an alternative grassland ecology. To test this inference, a two-dimensional finite-difference model has been constructed that includes parameterizations of the functions controlling feedback. Results of the experiment indicate that human-driven deforestation may shift regions of the Amazonian ecosystem to instability after 25%–30% of the forest has been permanently cleared, within two to four decades if the current practice is maintained. Even a temporary

* Corresponding author address: Dr. J. Alcock, Department of Environmental Sciences, The Pennsylvania State University, Abington College, Abington, PA 19001.
E-mail address: jea4@psu.edu

loss of the Amazon forest or significant portions of it would negatively impact terrestrial biodiversity.

KEYWORDS: Climate dynamics, evapotranspiration, hydroclimatology, precipitation, numerical modeling, South America

1. Introduction

Positive feedback has the potential to stabilize or destabilize a system (Milsum, 1968). It is, therefore, important to recognize systems controlled by positive feedback and to evaluate their resilience in the face of stress if we are to successfully predict system behavior (Hollings, 1973; Ludwig et al., 1997; Scheffer et al., 2001; Higgins et al., 2002). One approach to determining system resilience is to write an equation of state for the system that includes factors describing the multiple correlations or couplings among the variables that control feedback. Integration of the equation with respect to time and (or) with increasing stress allows one to predict the ability of the system to accept and recover from perturbation. Outcomes of such an analysis are likely to indicate consistent resilience of the system at all reasonable levels of stress or the catastrophic shift of the system to an alternative state (Ludwig et al., 1978, 1997; Wang and Eltahir, 2000; Higgins et al., 2002). A second approach to the problem is to use observed system behavior to identify resilient systems and those likely to experience a catastrophic shift in equilibrium (Done, 1992; Scheffer et al., 1993, 2001).

In this paper, a third approach is described: the use of graphical analysis to evaluate the effect of feedback on system resilience and to recognize conditions likely to produce shifts between alternative states. The advantage of this method is that generalized curves based on a qualitative description of the system are often sufficient for establishing a possible system response. Combined with finite-difference models that use parameterizations of couplings modeled during graphical analysis, this approach can provide important information about a system and its response to stress even when detailed mathematical descriptions of the system are not possible. An investigation of the effect of deforestation on the stability of the Amazon basin tropical forest ecosystem is used to demonstrate the method.

2. The Amazon basin ecosystem

Current practice in the Amazon basin is causing rapid changes to its tropical forest ecosystem. Most important are the agricultural, logging, and mining activities that cause permanent clearing of the forest at rates of about 0.5% yr^{-1} (Skole and Tucker, 1993; Nepstad et al., 1999). Simple models based on linear or even exponential extrapolations imply that the forest could withstand this assault on its viability for 150 to 200 years before its last vestiges were destroyed. However, these models do not consider the role of feedback among climatic, hydrologic, and biological processes within the ecosystem. Theoretical considerations suggest that this feedback has the potential to destabilize the system leading to a catastrophic system shift in the relatively near future.

Recognition of feedback between tropical forest and climate is not new (Salati et al., 1979), and a number of studies have been conducted to model the effect of deforestation of the Amazon basin on the regional and global climate (Shukla et al., 1990; Shuttleworth et al., 1991; Henderson-Sellers et al., 1993; Marengo et al., 1994; Bonell, 1998; Cox et al., 2000; Zhang et al., 2001). These studies, however, concentrate on the end-member case of total deforestation and so have not considered the reverse effect, the possible loss of tropical forest in response to climate change. This is important because the sustainability of the forest depends on a rather simple feedback between precipitation (P) and forest health (Wang and Eltahir, 2000; Alcock, 2001). The forest needs high levels of P for biological processes and to limit damage by fire (Nepstad et al., 1999; Cochrane et al., 1999; Cochrane, 2001; Nepstad et al., 2001; Siegert et al., 2001). A healthy forest returns a high percentage of P to the atmosphere through evapotranspiration (ET; Leopoldo et al., 1984; Marengo et al., 1994; Jipp et al., 1998). Deforestation can interrupt the cycle by reducing ET and increasing runoff (R) so that available water is lost to the local system. In addition, deforestation raises land surface and atmospheric temperatures, which, in turn, affects the dewpoint and local and regional convection patterns. Eltahir and Pal (Eltahir and Pal, 1996) report that the net effect of temperature and humidity changes over deforested land is to reduce local convective storms and to weaken intertropical convergence and thus reduce rainfall. The issue, however, is complicated by a new study that has found that temperature differences over pastures and forests are likely to cause small local convective storms (Baidya Roy and Avissar, 2002). The possible impact of this effect will be considered later in the paper, but is not considered likely to impact regional feedback patterns.

Figure 1 summarizes the processes and variables creating and affected by feedback in the system. With the exception of feedback involving temperature and intertropical convergence, all feedback loops are positive. That is, the algebraic product of all couplings in each loop is positive (Berner, 1999). Note that this definition is different from that used by Wang and Eltahir (Wang and Eltahir, 2000) who use positive and negative to be synonymous with enhancing and damping of perturbations, respectively. Using the algebraic product to determine the sign of feedback is preferable because it does not require prior knowledge of system behavior, nor does it allow the sign of a feedback loop to change as the strength of the coupling changes. Because most loops in Figure 1 are positive, and because the one negative loop involving temperature and intertropical convergence has been shown to be less important than the positive loop including absolute humidity and convergence (Eltahir and Pal, 1996), the overall effect of feedback between climate and forest is positive.

3. Graphical analysis

In order to further the analysis, the feedback presented in Figure 1 can be reduced to two functions (e.g., Figure 1b) so that graphical analysis can be used (e.g., Figure 2). Precipitation and leaf area index (LAI), a measure of forest health, have been chosen to represent the variables controlling feedback. In each case, multiple effects have been combined to create a single coupling. For example,

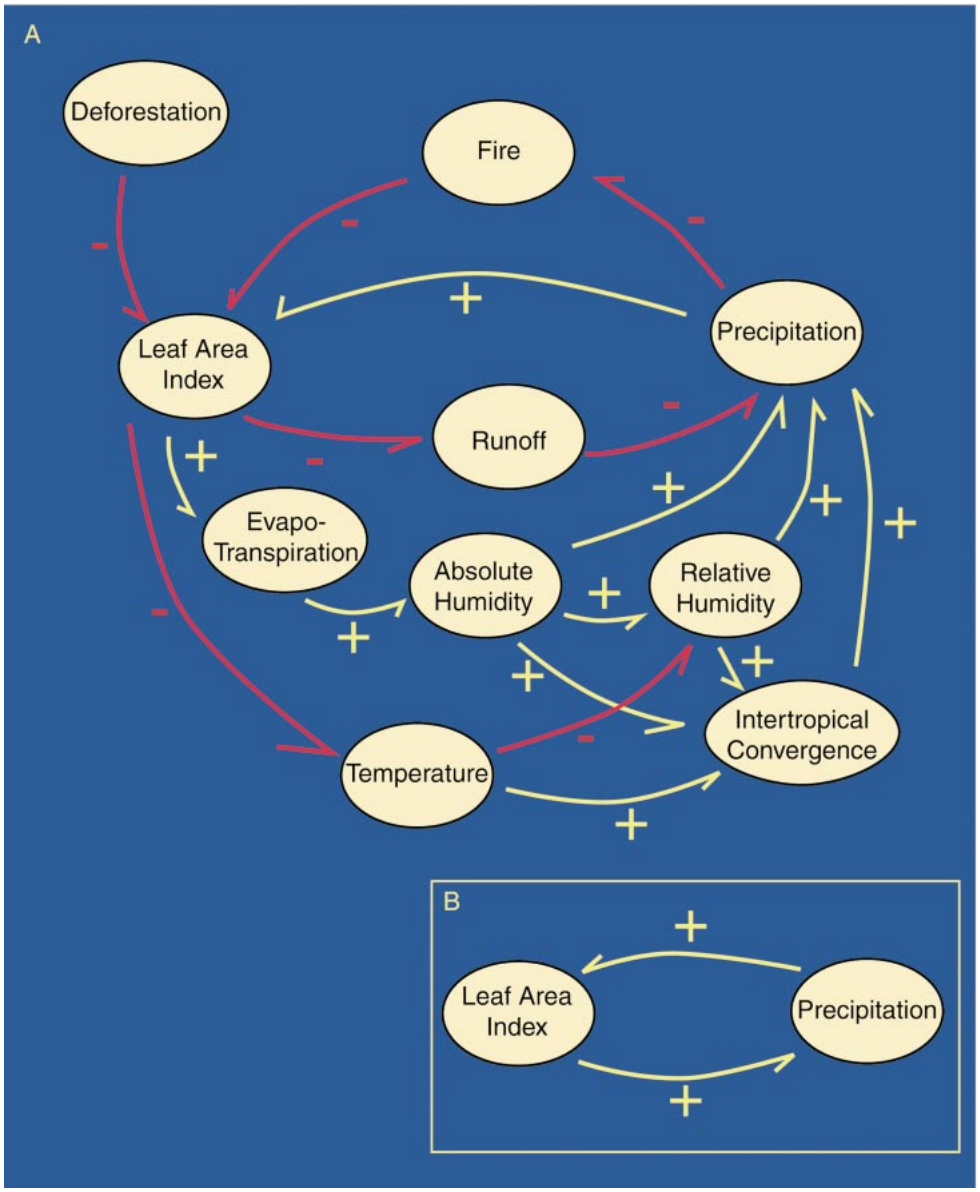

Figure 1. (a) Schematic diagram tracing feedback between forest and climate. The ovals contain variables that provide important measures of the state of the system. Arrows represent couplings, processes by which change in one variable affects a second. The sign of the arrow gives the sign of the slope of the function that describes the coupling. Feedback in the system is indicated by the closed loops that create a cyclical set of couplings. The sign of feedback is determined by the algebraic product of couplings in the loop. As discussed in the text, the net effect of the various feedback loops shown is to create positive feedback that controls system behavior. (b) For additional analysis, the feedback is reduced to a two-variable system with two couplings, each representing multiple processes.

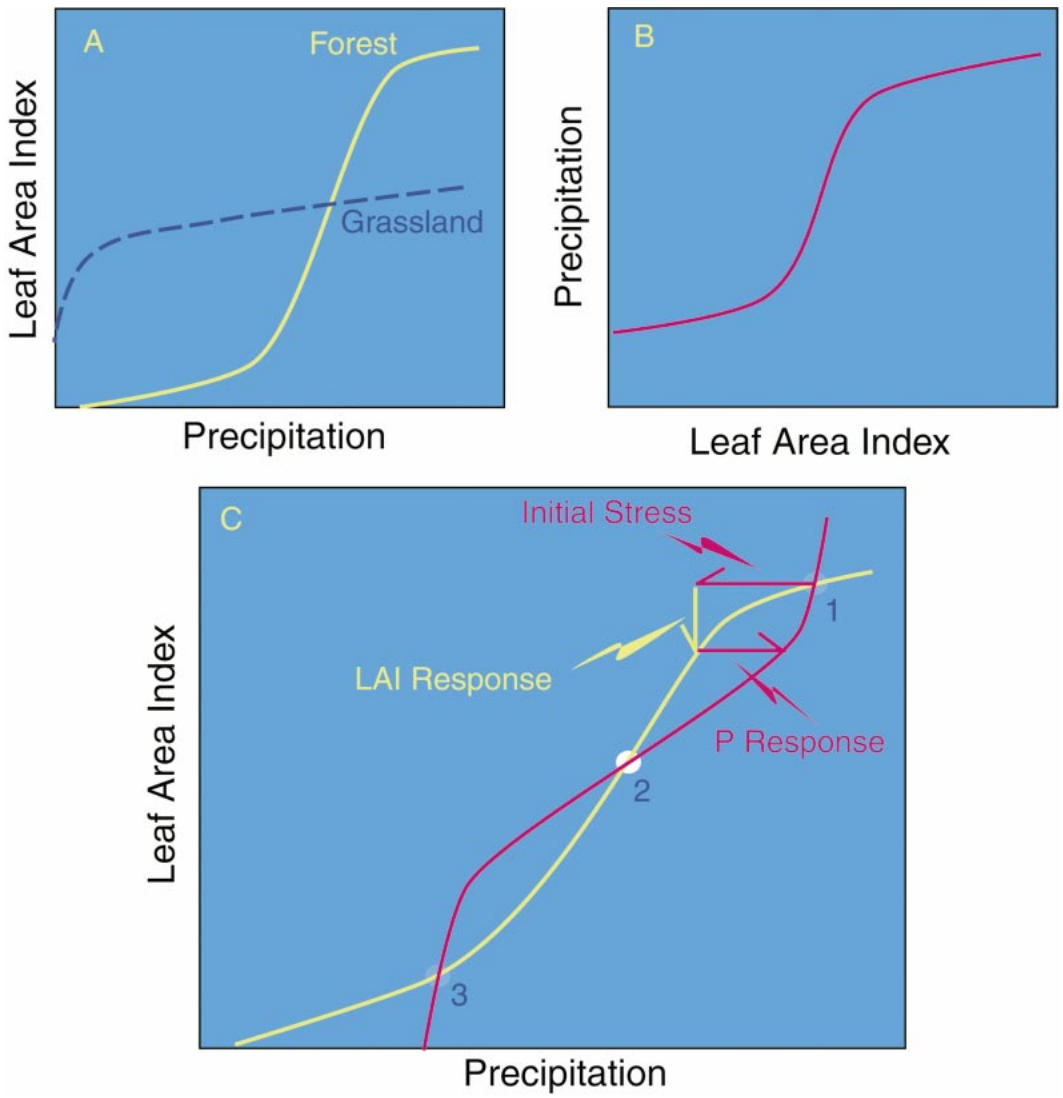

Figure 2. Schematic graphs showing possible mathematical expression of couplings in Figure 1b. (a) The effect of *P* on LAI for forest and grassland ecosystems. Precipitation *P* is measured in mm yr^{-1}. LAI is normalized with maximum LAI for a location that is set to 1 and with an allowable range between 1 and 0. The rationale for curve shapes is discussed in the text. (b) The predicted effect of change in LAI on *P*. (c) The two couplings are combined on a single graph to identify potential steady states (intersections of curves labeled 1, 2, and 3) and to allow stability of those states to be determined. The stepwise response of the system to deforestation at state 1 is traced by arrows and indicates that the system is resilient near state 1. Similar tests show state 2 to be unstable and state 3 to be stable.

the control of LAI by P includes both the direct effect of drought and the changing potential for fire as P changes.

In Figure 2, both couplings are presented as functions of the following form:

$$Y = \exp(-ax^2), \tag{1}$$

where a is a constant with a value greater than 1. Functions of this type produce a logistics curve with asymptotic approaches to maximum and minimum values. The representations are based on inference. For example, consider the effect of increasing P on LAI. As the forest becomes denser and various layers are more fully occupied, space limitations and nutrient availability become more important than P in controlling the expansion of LAI. Conversely, small reductions in P are likely to have little impact on forest health. More severe drought conditions would affect forest health by lowering the forest's resistance to disease, fire, and other factors, eventually leading to the replacement of forest vegetation. It seems probable that some vegetation would continue to persist despite severe drought, for example, in response to a local variation in soil moisture, and so LAI would also approach zero asymptotically. However, it is also possible that the response of LAI to severe drought approaches a linear function. Various forms of the function and its effect on the system's behavior will be considered later.

While the curves have been drawn to represent the tropical forest ecosystem, it should be recognized that alternative ecosystems with different feedback effects would replace the forest if it were to collapse. These alternatives—pasture land, savanna, or intermittent forest and grassland—would be described by a variety of curves similar to that drawn showing the effect of P on LAI for the forest. For this discussion, a second curve showing the grasslands' response to P has been included.

A similar curve is shown in Figure 2b representing the response of P to a change in LAI. At LAI = 0, a minimum level of precipitation will occur determined by intertropical convergence, local evaporation, and atmospheric temperature. As LAI increases, climatic changes and increased ET can produce a rapid increase in precipitation. At high LAI, relative humidity in the forest approaches 100% and little additional water vapor can be added to the atmosphere. Precipitation change with increasing LAI diminishes. Studies of the regeneration of forests have found that ET increases most rapidly in the first few years of forest regrowth and that a change in ET follows a curve similar to that shown in Figure 2b (Murakami et al., 2000).

Because graphs in both Figures 2a and 2b concern the same variables, it is possible to combine the graphs (i.e., Figure 2c) and to use the combined graphs to evaluate the system's response to perturbations. As drawn, the forest–climate system has three steady states identified by the points of intersection. Intersections are the only states in which conditions satisfy both functions; therefore, they are the only states at which the system can achieve equilibrium. All other states require that at least one of the couplings must act to change the conditions of the system.

Stability of the steady states can be evaluated visually by introducing a stress to the equilibrium system. For example, a temporary decrease in P when the system is at state 1 (initial stress) will result in a small decrease in LAI. LAI

remains high enough to allow partial recovery of *P* to near-original levels. Higher *P* will in turn allow partial recovery of LAI. Eventually the system will return to state 1 and thus is stable in the area of state 1. The model, therefore, predicts a resilient system at high levels of *P* and LAI. This has been the condition of the Amazon basin forest as the ecosystem has maintained equilibrium (Salati and Vose, 1984) and has even been able to expand at its margin during the last several millennia (Mayle et al., 2000).

State 2 is unstable. A decrease in *P* at state 2 results in a large decrease in LAI, and lower levels of LAI lead to additional loss of *P*. State 2, therefore, can be seen as a point-of-no-return for the system. Should current deforestation in the Amazon basin move the system to state 2, then any additional clearing or temporary decrease in *P* would result in the collapse of the ecosystem and a shift toward an alternative ecosystem at state 3. The loss of system resilience at state 2 is possible even though the forest is currently controlled by stable state 1 because the forcing process is continuous and the recovery of the system through regrowth is slow relative to the rate of clearing.

This first pass at graphical analysis, therefore, leads to two important conclusions. The model as presented is consistent with current system behavior in that it predicts a stable system with high LAI. Second, the model predicts that continued forcing may move the system beyond a point-of-no-return leading to a catastrophic ecosystem shift.

As noted above, the tropical forest is not the only ecosystem that might develop within the Amazon basin. Grasses are likely to be the first plants to replace cleared forest, especially if clearing is intended for agricultural purposes or if it occurred in response to drought as grasses require less water. If we include a grassland ecosystem in the model (Figure 3), it provides an alternative to the unrealistic creation of barren or near-barren ground at state 3. As drawn, the grassland ecosystem produces only a single steady state because grasses are likely to grow well even at minimum levels of *P* in the Amazon basin. Because state 1g is stable, the system will naturally shift to state 1g should the forest ecosystem collapse. The position of state 1g relative to state 2f, the point-of-no-return for the forest ecosystem, will determine the ability of the forest to recover after collapse if human intervention is controlled. If the grassland equilibrium state is at state $1g^1$ (Figure 3) so that *P* is greater than *P* at state 2f, the grassland ecosystem will be temporary and the forest will return if human interference (deforestation) is halted. The model of Wang and Eltahir (Wang and Eltahir, 2000) predicts recovery of the African tropical forest from a catastrophic but temporary perturbation causing total forest loss and so would be consistent with grassland equilibrium at state $1g^1$. However, if grassland stabilizes the system at state $1g^2$, then a permanent shift from forest to grassland ecosystems would occur.

3.1 Quantifying the model

Although the model presented is reasonable, it does not necessarily reflect actual system behavior. It is possible to estimate mathematical functions that define the couplings, that is, to create a parameterized model of the system. If this is done, a different outcome may result. Curves drawn based on the parameterizations are

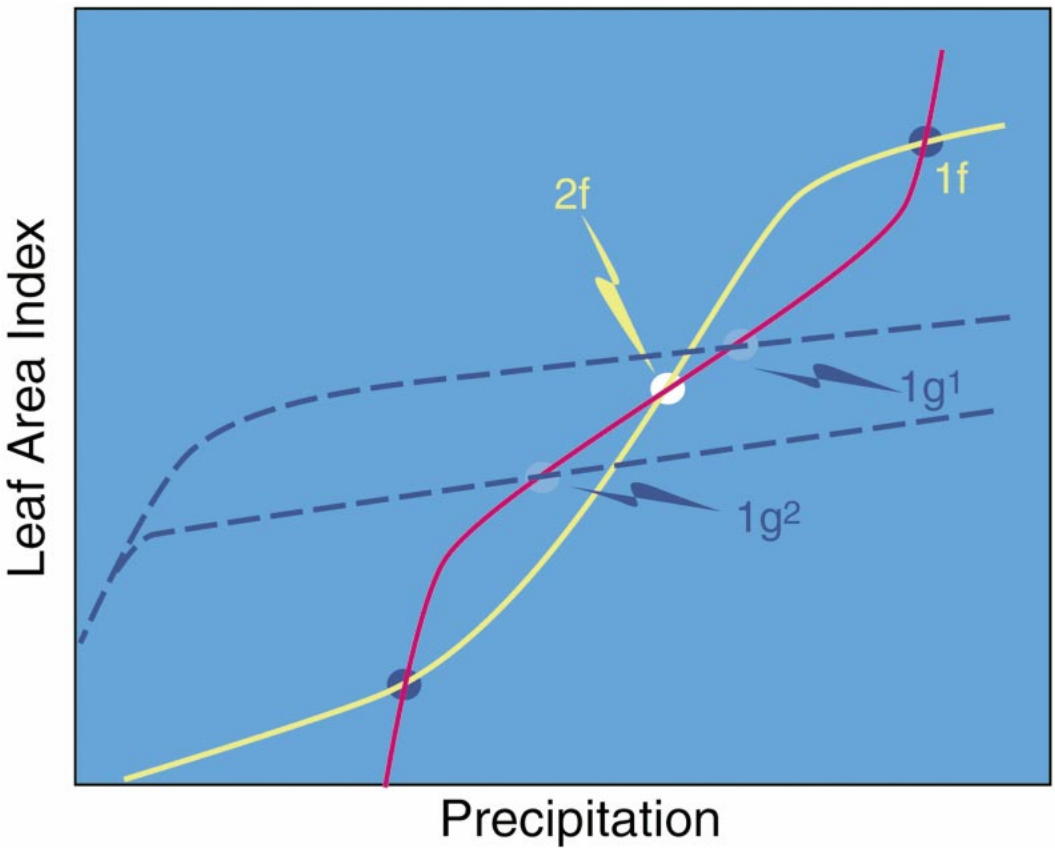

Figure 3. Figure 2c has been modified to predict the effects of the grassland ecosystem on the resilience of the forest. In addition the effect of *P* on LAI of grassland suggests that the forest may regrow after the ecosystem shifts if stable grassland state is at $1g^1$ with *P* greater than *P* at the unstable forest state 2f. Recovery of the forest depends on a cessation of actions that might clear new forest growth.

shown in Figure 4. The results indicate that either one or three steady states may exist in the tropical forest depending on the shape of the functions that control system behavior. A single steady state would also be consistent with the model of Wang and Eltahir (Wang and Eltahir, 2000) because with a single stable steady state, the forest must always recover from stress, even from total loss of the forest, which occurs in their model.

However, the current situation in the Amazon basin is distinct in that deforestation is not a temporary, but a constant stress that produces a permanent change. Approximately 0.5% of the forest is permanently cleared each year and as clearing proceeds, the possible LAI maximum for the basin is reduced. This has the effect of changing the position of the curve, LAI = $f(P)$ (Figure 5) causing the position of stable state 1 to shift to lower values of LAI and *P*. Eventually this leads to the loss of state 1 (Figure 5a) or the loss of states 1 and 2 (Figures

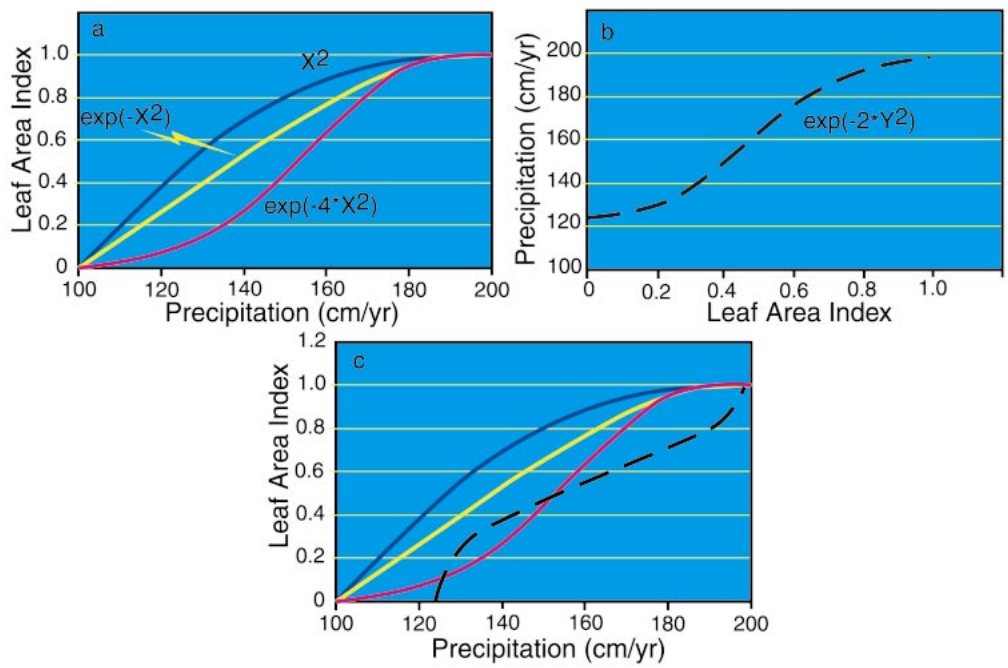

Figure 4. Parameterizations of couplings between LAI and *P*. (a) Three possible functions are used to predict the effect of *P* on LAI. (b) A logistics curve used to describe the effect of LAI on *P*. (c) Functions are combined to create a single graph. Colors and patterns are the same as those used in (a) and (b). Only the magenta curve showing the effect of *P* on LAI creates a three-steady-state system similar to that shown in Figure 2c. Blue and yellow curves predict that the system will maintain resilience under all conditions considered.

5b and 5c) and shifts equilibrium conditions to a new state at low *P* and low LAI. Because recovery of temporary clearings is slow relative to the rate of clearing, the actual shift to state 3 occurs more rapidly than is predicted by considering only the permanent clearing of the forest.

3.2 A finite-difference test of graphical analysis

The results of this graphical analysis have been tested by a finite-difference model written in Excel Visual Basic that is based on the parameterizations discussed above. Figure 6 presents a flowchart describing the program's algorithm. (A copy of the program may be obtained from the author.) A more complex model that combines advanced climate models with land surface and biome response to climate change (Brovkin et al., 1998; Dolman et al., 1999; Wang and Eltahir, 2000; Baidya Roy and Avissar, 2002) might also be used, but is beyond the scope of this paper.

The finite-difference model follows changes in the system that occur at nodes within a 100 × 100 or 250 × 250 grid in response to clearing. A fixed number

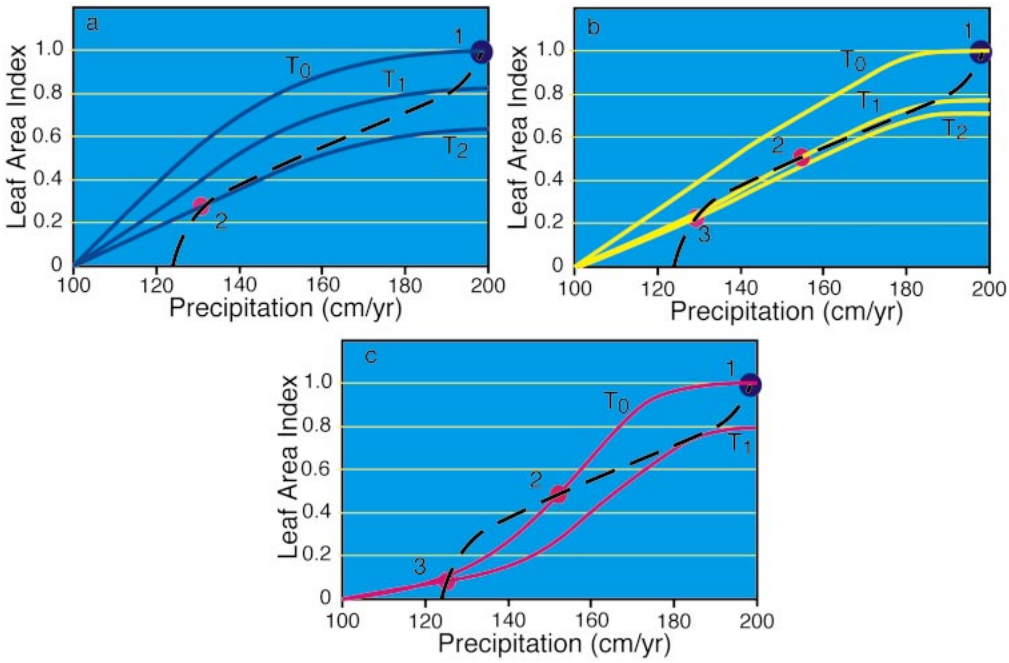

Figure 5. The effect of permanent clearing of the forest on system behavior is illustrated. Replacement of forest by pasture causes a permanent decrease in LAI and so causes curves showing the effect of *P* on LAI to shift to lower LAI values at any *P*. The result in each case forces a shift to low LAI and *P* representing a catastrophic replacement of the forest by an alternative ecosystem. Colors and patterns are the same as those used in Figure 4.

of nodes are cleared each year by a random function that favors clearing near previously cleared nodes. A fixed percent of previously cleared nodes are also recleared leading to a permanent clearing of 0.5% yr^{-1} in most model runs. If deforestation causes the system to collapse, human-driven deforestation is stopped in most experiments, and the model system is allowed to establish a new equilibrium. Alternatively, permanently cleared lands were maintained to test the effect of this more realistic possibility on the potential recovery of the forest.

Forest loss also occurs in response to drought. Loss is calculated as occurring in an exponential fashion between 90% and 50% of initial *P* at which point all trees would succumb to drought conditions. Other model parameters prevent *P* from falling below about 65% of initial conditions; thus, this ultimate limit on forest existence is not reached.

Regrowth of vegetation is modeled as the forest with the same properties as the original forest relative to its effect on *P* or as a second vegetation type representing a savanna-like ecosystem with lower values of ET and other climatic effects that reduce *P*. Precipitation determines which vegetation type grows at a particular node with the savanna being more resistant to drought; thus, it is the

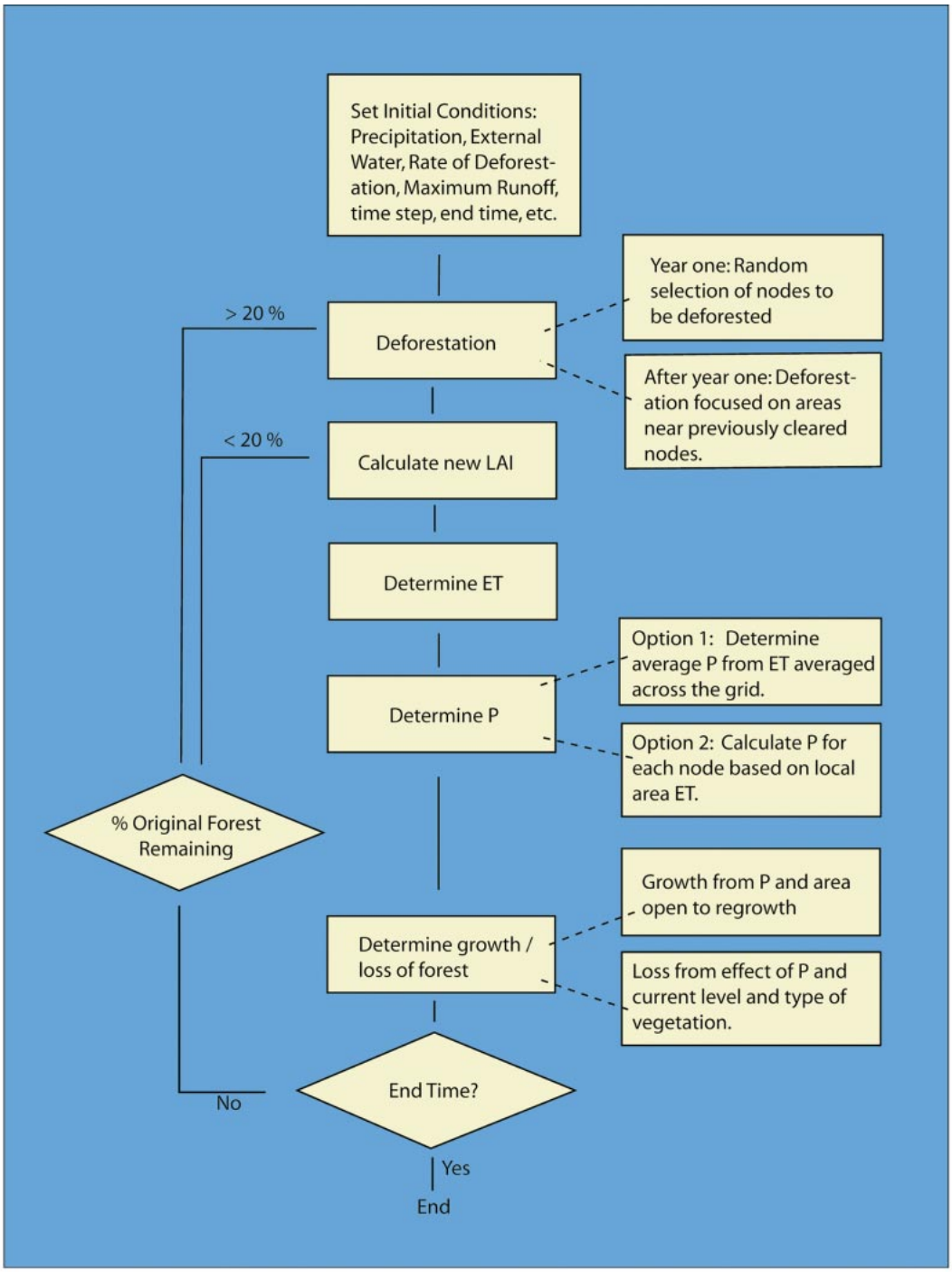

Figure 6. Flowchart presenting the algorithm used to construct the finite-difference model of feedback between climate and forest in the Amazon basin.

dominant type at low levels of *P*. Grasses are also modeled as the first species to grow on cleared land and are assumed to have fully colonized a node 2 yr after clearing.

The forest in turn acts to control *P* by returning a large percentage, 50%–80%, of rain to the air through ET (Leopoldo et al., 1984; Marengo et al., 1994; Jipp et al., 1998) and through its impact on the local climate. Water not returned to the atmosphere by ET is lost to the system, as indicated by a typical water balance equation for the tropical forest:

$$R = P - \mathrm{ET} \tag{2}$$

(Marengo et al., 1994). Soil water, not included in the equation, can also serve as an important reservoir or sink in a stressed system. Trees have been shown to extend their root systems as the water table recedes in response to hydrometeorological change (Jipp et al., 1998) and would add water to the system. Should a forest be cleared, the deeper soil water would no longer be accessible, and recharge of the deeper soils will remove available water from the system.

Eltahir and Bras (Eltahir and Bras, 1994) present an alternative model and determine that only approximately 25% of rain in the Amazon basin is recycled water returned to the atmosphere by ET. Their model (Figure 7) still recognizes that nearly 60% of *P* is returned to the atmosphere, but they conclude that a significant portion of that moisture is carried out of the basin by atmospheric circulation. These data raise an important question about the impact of decreases in ET on *P*. The experiments described here assume that a reduction in ET has an equivalent effect on *P* because it decreases absolute and relative humidity of the atmospheric system. In effect the finite-difference model assumes that water vapor leaving the basin remains constant, an assumption that may not be valid if airflow through the system is decreased by reduced intertropical convergence or if higher temperatures allow the air leaving the system to carry more moisture.

Precipitation in the model is determined by a time step calculation of external water entering the system and a measure of ET and climate conditions affecting *P* at each node based on the amount and type of vegetation. External water is set by the initial conditions of the program as equal to initial *R*, a condition required by Equation (2). Climatic conditions and lowered ET over fully developed grasslands are modeled to reduce *P* by about 15%, a conservative estimate when compared to the about 20% decrease in *P* predicted by the most recent study of the climatic effect of complete deforestation of the basin (Zhang et al., 2002). Cleared land without vegetation returns a fixed minimum amount of water to the atmosphere representing simple evaporation. Actual *P* at each time step is then determined based on an average ET for the entire grid or for a subarea of the grid surrounding each node. The two approaches allow one to explore the effect of different degrees of atmospheric mixing on model outcomes.

A review of *P* and vegetation type indicates that 1600 mm yr^{-1} is an approximate minimum value for rainfall required to sustain the forest, although seasonality of rainfall is an important secondary factor (Hoare, 1998; Mathews, 1983). Rainfall is higher in much of the Amazon basin at 2000–2500 mm yr^{-1}

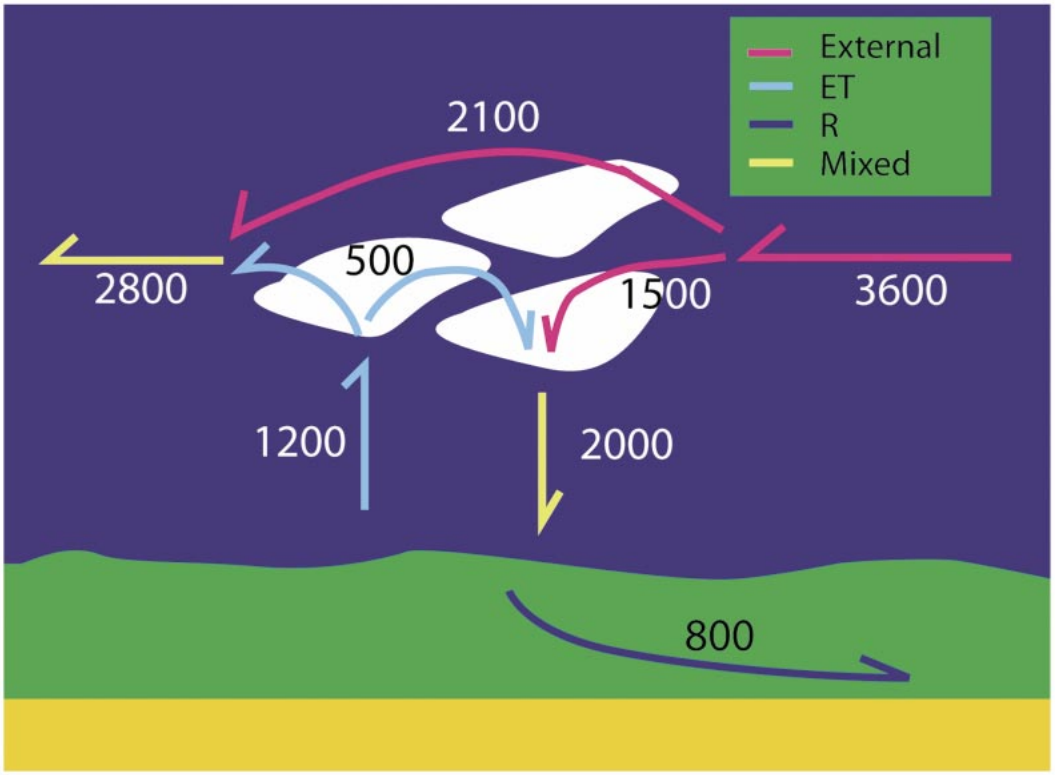

Figure 7. A schematic representation of influx and outflow of water vapor as it affects precipitation and runoff. The model is presented to be consistent with the data of Eltahir and Bras (Eltahir and Bras, 1994) and to produce $P = 2000$ mm yr^{-1}.

(Marengo et al., 1994). Therefore, initial P was set at 2000 mm for most experimental runs.

One additional variable, the rate of deforestation, is important to the system but external to feedback. Rates of deforestation in the Amazon basin have been estimated to be 0.4% to more than 2.0% yr^{-1} (Skole and Tucker, 1993; Nepstad et al., 1999). The increase in visibly deforested land as seen in Landsat images is about 0.5% yr^{-1}, indicating that these lands are recleared on a regular basis. Combining satellite analysis, field observations, and interviews of landowners, Nepstad and others (Nepstad et al., 1999) estimate that an additional 0.5% is cleared each year but not as permanent clearing. Forest is also lost to fire at a rate that may be equal to or possibly greater than direct loss to human actions, especially during drought (Nepstad et al., 1999; Cochrane et al., 1999; Cochrane, 2001; Nepstad et al., 2001).

3.3 Experimental results and discussion

One must recognize that any model of a system as complex as the Amazon forest will be limited in its ability to fully recreate the system as a mathematical reality.

This is especially true of a model such as the one used in the experiments described here that relies heavily on parameterizations of complex processes to make predictive statements about future system behavior. However, the very simplicity of the model derived from the parameterizations can be a strength because it allows a rapid and clear definition of important processes and their potential to affect the system. The robustness of the model results can be tested by allowing initial conditions and parameterization of processes to vary across a range of potentially reasonable values. If the model response remains constant or similar as variables and functions describing processes change, the confidence in the model predictions increases so long as the underlying assumptions of the model are valid.

Table 1: Initial conditions for model runs.

Variables set at model initiation	Variable tested in multiple runs						
	Years of clearing	Initial *P*	*P* causing first loss of forest	*P* causing total loss of forest	Clearing rate	External water	ET potential of secondary vegetation
Years of clearing	55*(5)**	Until collapse	Until collapse	Until collapse	Until collapse	Until collapse	Until collapse
Clearing rate	0.01	0.01	0.01	0.01	0.006* (0.002)**	0.01	0.01
Percent of cleared lands recleared each year	50	50	50	50	50	50	50
External water as fraction of initial *P*	0.45	0.45	0.45	0.45	0.45	0.35*(0.1)**	0.45
Initial *P* (cm yr^{-1})	200	200*(50)**	200	200	200	200	200
ET of secondary vegetation as fraction of forest potential	0.7	0.7	0.7	0.7	0.7	0.7	0.*0.1)**
Rate of growth of secondary vegetation (yr to full potential)	2	2	2	2	2	2	2
Maximum runoff (% of initial *P*)	75	75	75	75	75	75	75
Initial loss of vegetation at fraction of initial *P*	0.90	0.90	0.85* (0.05)**	0.90	0.90	0.90	0.90
Total loss of forest (% of initial *P*)	50	50	50	50*(10)**	50	50	50
Growth rate of forest (yr to full potential)	25	25	25	25	25	25	25
Run time (yr)	100.0	100.0	100.0	100.0	100.0	100.0	100.0
Time step (steps yr^{-1})	5.0	5.0	5.0	5.0	5.0	5.0	5.0

* Value of tested variable in first run.
** Incremental change in variable in additional runs.

Results of eight sets of representative experiments are summarized in Figure 8. Most model runs that do not arbitrarily halt human-generated deforestation before collapse predict ecosystem collapse between 25 and 100 yr of the onset of rapid deforestation. With conservative estimates of variables and parameters

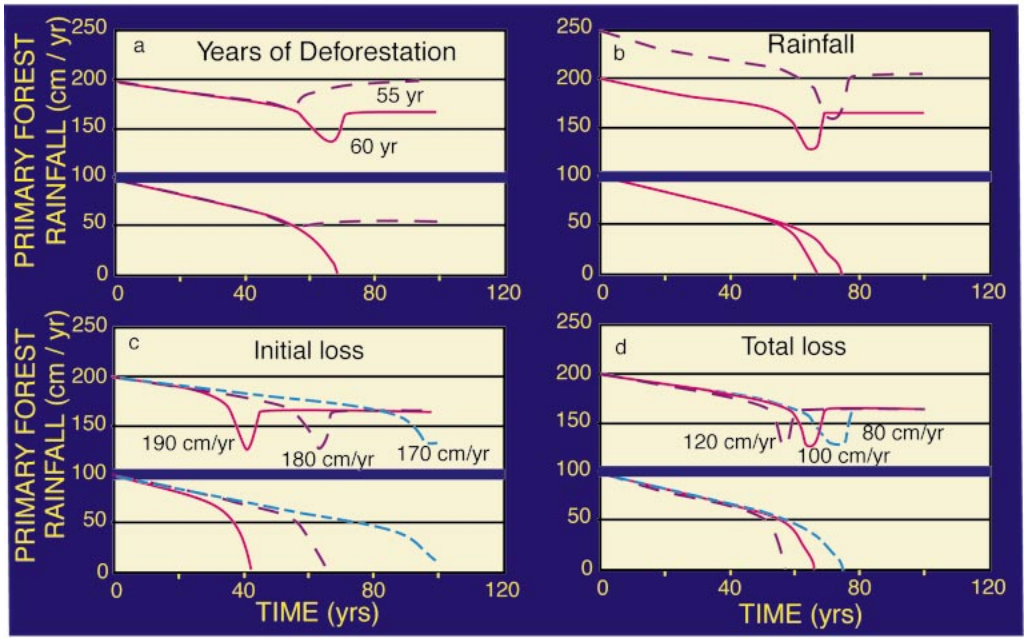

Figure 8. Results of eight series of model runs testing the impact of changes in important variables and parameterizations of feedback. Initial conditions are listed in Table 1. (a) Effect of arbitrarily halting human intervention after 55 and 60 yr. The result supports the implication of graphical analysis that the system, although currently stable, has the potential to switch to an alternative mode of behavior. Catastrophic shift in the ecosystem occurs shortly after marked change in slope of curves showing *P* and undisturbed primary forest. Area of forest that has been permanently cleared will approximate time divided by 2. (b) Initial *P* is changed from 2000 to 2500 mm yr^{-1} with a small impact on model outcome. (c) Model results when *P* that allows forest damage is varied between 1700 and 1900 mm yr^{-1}. (d) Minimum *P* required to allow some forest is varied from 800 to 1200 mm yr^{-1}. (e) Impact of changing rates of deforestation are shown. (f) The effect of pasture on *P* is varied between 85% and 95% of *P* over forest. (g) The effect of different functions used to describe couplings on model outcomes. Curve 1 experiment used $P\alpha\ \exp[-4(1 - \mathrm{LAI})^2]$; curve 2, $P\alpha\ \exp[-2(1 - \mathrm{LAI})^2]$; and curve 3, $P\alpha\ \exp[-1(1 - \mathrm{LAI})^2]$ with Equation (4) to model forest loss. Curve 4 experiment sets the loss of forest as $\alpha\ \{[(180 - P)/180]^2\}$ and *P* (cm) controlled by Equation (3). Note that colors and patterns do not correspond to those used in Figures 4 and 5. (h) Model effects of limited atmospheric mixing across 2.5% and 25% of grid area on the ecosystem's response to deforestation compared to mixing across the entire system. The model used for these calculations was based on an early version of the program that used exponential responses and allowed initial damage at 95% *P*. Experiments were not rerun because each run required several weeks to complete. Alternative parameterizations would change the years to collapse, but not the nature of the outcome.

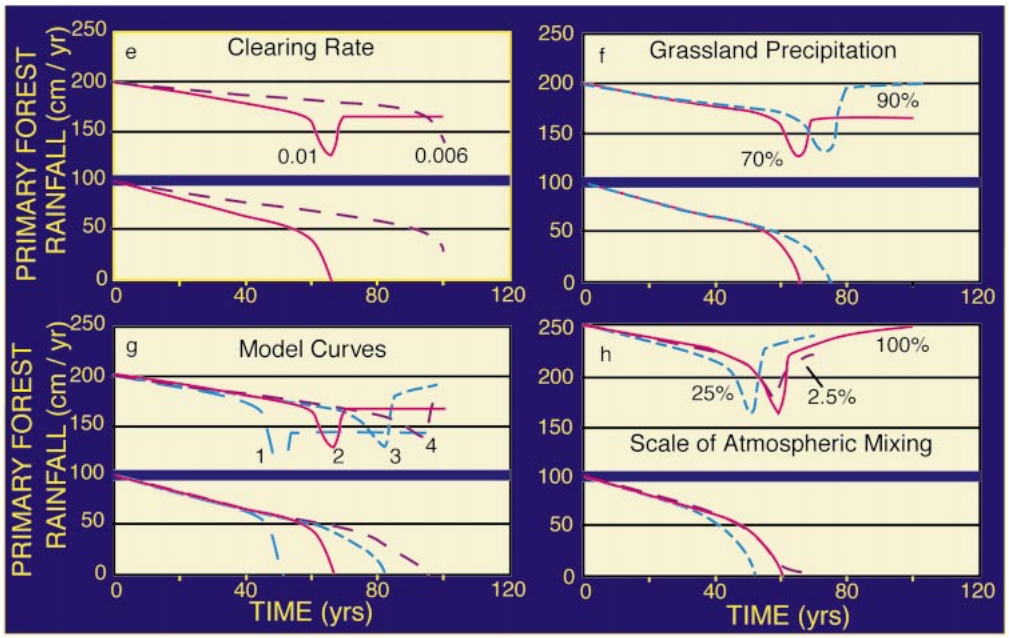

Figure 8. (*Continued.*)

(see Table 1) the system loses resilience after about 60 yr of deforestation or after about 30% of the model forest has been permanently cleared. Loss of the remaining model forest is rapid, occurring within about 5 yr. If human intervention in the ecosystem ends after collapse, then the forest ecosystem may regrow. However, if intervention continues, even if it is limited to maintaining previously cleared lands, the grassland ecosystem becomes permanent. A few experiments that delay initial feedback response to relatively low levels of *P*, or that use a weakened feedback response, do not predict catastrophic system change.

In each set of model runs, a parameter or controlling variable was varied across a range of reasonable values to test the robustness of the model with respect to that variable. Each experiment is described briefly.

3.3.1. Precipitation and its impact on forest resilience

In most runs initial *P* was set at 2000 mm yr^{-1}, a value considered to be a reasonable approximation of average rainfall within the Amazon basin. However, because measured rainfall varies across the Amazon forest from about 1600 to more than 3000 mm yr^{-1} (Marengo et al., 1994), *P* was increased to 2500 mm yr^{-1} to test the effect of the initial level of precipitation on the model. No other changes were made. For example, initial loss of forest began at 90% of initial *P* and total loss occurred if *P* fell to 1000 mm yr^{-1}. This assumes that the forest at any location has evolved to be in balance with and to use available moisture (Bazzaz, 1998). It is possible that stress on a forest by continued drought might result in changes to species that require less water. However, the relatively rapid

nature of the changes that are occurring is unlikely to allow what must be a gradual process of species replacement. A change in initial *P* does not significantly affect model outcomes (Figure 8b).

Experiments also tested the effect of changing the minimum decrease in *P* that would cause loss in the forest and the level of *P* at which all trees would be lost (Figures 8c and 8d). Published data that quantify the effects of drought on the forest were not found. However, data are reported that indicate a strong seasonal response of LAI to precipitation (Santos and Negri, 1997), the loss of forest near cleared land (Laurance et al., 1997; Cochrane et al., 1999; Nepstad et al., 2001; Cochrane, 2001), and the effect of climatic change caused by deforestation on uncleared forests (Lawton et al., 2001). In most runs, the model forest began to experience some natural loss if *P* fell to 90% of initial values. An actual decrease in forest health as measured by change in LAI did not occur until *P* was less than 90% of its initial value because loss is balanced by a growth factor. Forest resistance to drought was varied so that natural loss began if *P* decreased to 85%, 90%, or 95% of initial *P*. Increased resistance to drought enhances the resiliency of the forest and thus delays the ecosystem's collapse.

Minimum values of *P* required to sustain some forest were varied from 40% to 60% of initial *P* with most experiments run at 50% (Figure 8d). Because the model system constrains minimum amounts of ET and external moisture entering the system, *P* never falls below about 65% of initial *P*. Change in this variable reshapes the function controlling the loss of vegetation to drought and thus affects the model's response; however, the effects are small.

3.3.2. Effects of clearing rates

The model includes two kinds of clearing of the forest: clearing of virgin lands and reclearing previously cleared nodes to established permanently cleared lands. In most runs the former occurred at a rate of 1.0% yr^{-1} and the latter at 0.5% yr^{-1} with values set to mimic measured rates of deforestation (Nepstad et al., 1999). Changing either variable will change the years before the ecosystem's collapse (Figure 8e), but as would be expected they do not have much impact on the conditions resulting in the loss of system resilience. In each of these experiments, a catastrophic shift in the model ecosystem occurs when 25%–30% of the forest has been permanently cleared to pasture.

3.3.3 Effect of grassland on precipitation

The effect of grassland on *P* is set so that *P* above grassland was about 85% of *P* over forest, a value consistent with, but slightly higher than, most predictions from GCMs that have considered the effect of complete deforestation on the Amazonian climate (Shukla et al., 1990; Shuttleworth et al., 1991; Henderson-Sellers et al., 1993; Marengo et al., 1994; Bonell, 1998; Zhang et al., 2001). To evaluate the impact of this parameter on model results, the *P* over grassland was varied between 85% and 95% of a mature forest. Although this variable has little impact on the ability of the forest to withstand the effects of deforestation, it does affect the ability of the forest to regenerate itself if human interference is halted

(Figure 8f). This is consistent with the qualitative model derived from graphical analysis and presented above.

3.3.4 Functions defining feedback

The years to loss of resilience are strongly correlated with the function used to describe the forest's response to precipitation. As predicted by graphical analysis, a simple exponential function slows the system shift relative to a response that follows a logistics curve (Figures 4, 5, and 8g). For most model runs, the logistics curves were used on the inference that they better fit reality as discussed above. Furthermore, the typical forms of the equation were

$$P \alpha \exp[-2(1 - d)^2] \text{ and} \tag{3}$$

$$\text{loss } \alpha \exp[-1(l^2)], \tag{4}$$

where d is a measure of the transpiration potential of the vegetation-combining type, amount, and climatic impacts; loss is the loss of vegetation from a particular node; and l is a measure of P relative to the P needed to preserve a healthy forest. The most common model, therefore, resembles the graphical analysis presented in Figure 5b, which treats the loss of forest in response to drought as nearly linear at low P. This choice of parameterizations is conservative relative to a well-developed logistics curve with an asymptotic approach to minimum LAI, as suggested by the analysis above. The importance of the form of the parameterizations, visible in these results, indicates that observational data that better describe the mathematical relationships between P and LAI and LAI and P are needed to accurately predict the future behavior of the ecosystem.

3.4 Other issues

3.4.1 Scale

The 100 × 100 or 250 × 250 grid of the model forest has not been scaled to represent actual distance. The grid, therefore, might be taken to represent either the entire Amazon basin or an area within it. If the distance between nodes were set at 5 km, then the smaller grid would cover 250,000 km^2 or approximately one-sixteenth of the basin. At this scale, the total area represented approximates the area of a node in the GCM used by Marengo et al. (Marengo et al., 1994) or an area equal to about one-eighth of the larger catchments of the southern and western basin (Marengo et al., 1994). In the larger grid a distance of 2 km between nodes covers the same area. A distance of 1 km between nodes in the larger grid creates an area of 62,500 km^2 or about 4% of the catchment area of the Madeiras River.

A smaller model area is more likely to mimic the behavior of the forest because a smaller area is likely to be more homogeneous in response than a larger one. Important differences are created by the variations in seasonality of precipitation and in the positions within or external to river flood plains that experience seasonal flooding. However, too small an area might lead to a misrepresentation of climatic effects that involve large-scale and local atmospheric mixing.

3.4.2 Area of atmospheric mixing

Although the model is dimensionless, two distinct scales are used to measure the model change within the system. Growth and loss of forest and the resultant changes in LAI and ET are measured at the scale of individual nodes. Because these changes would operate on the scale of individual trees, they should be measured across the smallest possible area. Precipitation change is calculated from either LAI as measured across the entire grid or in smaller sections of the grid centered on each node as *P* is determined for that node (Figure 8h). Smaller sections represented 0.6%, 2.5%, and 25% of the model area. The two different approaches represent two end-member models of the processes controlling precipitation in the Amazon basin. Averaging LAI and ET changes across the entire grid infers rapid and large-scale atmospheric mixing within the zone of intertropical convergence. Averaging across subareas infers that local *P* results from local convective storms. Both processes are active in the Amazon (Eltahir and Pal, 1996).

Calculating *P* across subregions of the model does produce a different result from models that average ET across the entire grid. Loss of resilience occurs more rapidly when mixing occurs across 25% of the grid. This is probably a result of concentrating the effects of drought near areas that have experienced deforestation. Because both large-scale mixing and local convective storms contribute to basin *P*, it may be that this model, which includes the moderate mixing of atmospheric moisture, best represents the ecosystem's reality.

Models that limit atmospheric mixing to less than or equal to 1% of the model area limit collapse to areas near deforested nodes. This raises the possibility that small areas of undisturbed forest may be preserved if atmospheric mixing of water returned to the atmosphere occurs on a relatively small scale. Reports that the majority of damage to the forest occur within 1 km of previously deforested areas (Cochrane, 2001) suggest that local climatic changes may be important; however, the forces that act to concentrate damage are varied, including the concentration of human interventions, so the impact of climatic change remains uncertain. Determining regional and local contributions to *P* as the ecosystem changes is important because the ability of the forest to prevent large-scale extinction and loss of biodiversity depends on their not being destroyed in the general ecosystem collapse predicted by most model runs (Turner and Corlett, 1996; Phillips, 1997).

3.4.3 Effects of local climate change

Baidya Roy and Avissar (Baidya Roy and Avissar, 2002) have constructed a model that explicitly considers the local (kilometer scale) changes in weather patterns caused by a change in land cover within the Amazon basin that results from deforestation. They conclude that the warmer temperatures above deforested areas will increase small convective storms and move moisture from the forest to pasture lands. The impact of such local changes, if they occur, on the broader problem of the forest ecosystem's resilience is uncertain. First, an increase in *P* on permanently cleared land will not enhance regrowth of forest. Second, a shift of moisture from the forest to these permanently cleared lands will reduce *P* over

the forest and possibly enhance damage to the forest. Third, reports of increased wind damage to trees near cleared patches are inferred to be a result of small convective storms (Laurence et al., 1997) such as those that form in the model of Baidya Roy and Avissar (Baidya Roy and Avissar, 2002). Damage at the forest–pasture boundary could be an additional positive feedback leading to the increased loss of the forest.

3.4.4 Changes in area water balance

Three factors may alter water balance within a region of the basin: change in water leaving the system as runoff and atmospheric moisture, change in external water vapor entering the system, and change in available soil water. Increases in runoff caused by the clearing of land, which allows a more rapid movement of water to and across the ground surface, remove moisture from an area. Similarly, warming of the basin may lead to increased loss of moisture as water vapor leaving the system because the dewpoint has been increased. Once lost, the water-balance deficit can be reduced only if there are increases in water from some other source. For example, additional moisture from external sources may enter the region during periods of strengthened intertropical convergence. Variability of P in the basin can be large, about $\pm$ 50% of the average values in Pará (Jipp et al., 1998). Increased P could restore lost water. Of course, lower than average P would exacerbate the water-balance problem. Eltahir and Pal (Eltahir and Pal, 1996) predict that deforestation by reducing absolute humidity will reduce large-scale convective forces and thus weaken intertropical convergence. They suggest that this feedback may be largely responsible for decreases in P in a deforested Amazon basin, which are predicted by GCM experiments.

Soil water is also an important potential reservoir and sink for water. Immediately after deforestation, it should act as a sink as the deep sources of water available to trees will not be available to grasses and initial forest regrowth (Jipp et al., 1998). Recharge of the deeper ($>$ 2 m) soils will act to remove water from the system and so might potentially cause additional reduction in rainfall. If a secondary forest grows and matures, this water would become available and begin to be recycled through ET. This could serve as an important feedback allowing regeneration of forest if human-driven deforestation is controlled.

3.4.5 Position within the basin

The model described here assumes 45% of P is derived from external moisture entering the system, which is consistent with an estimated total R as a percent of P for the entire basin (Marengo et al., 1994). Runoff from individual major catchments ranges from 30% to 50% of P. Higher values are typically associated with areas of topographic uplift. One might also expect that areas near the Atlantic would receive more external moisture as a percent of P, but this does not appear to be supported by observed R. This would suggest that surface conditions—surface gradient in undisturbed forest and vegetative cover in disturbed areas—are primarily responsible for controlling R. If this is the case, then the model presented here should apply equally to all areas of the Amazon basin. If coastal

areas are in fact less susceptible to drought induced by deforestation, then the model results should only be applied to interior portions of the basin.

Perhaps more important is the position of the forest within or external to areas that are regularly flooded. Flooding would recharge the soil water reservoir and so provide the forest with an additional source of water that might make it more resistant to decreases in local *P*. If this is the case, then forests located in floodplains may not respond to deforestation-induced climate change as predicted by the model.

3.4.6 Application to other climate–biome interactions

The model described here has attempted to predict the behavior of the Amazon basin's ecosystem to current stress caused by deforestation. Other ecosystems might also be at risk. For example, atmospheric–vegetation interactions in the Sahel have been modeled and indicate that it may also be controlled by positive feedback that creates multiple behavioral states (Brovkin et al., 1998).

4. Conclusions

Qualitative models that combine descriptions of feedback and graphical analysis can provide valuable insight into the functioning of complex systems. Especially interesting is the potential for systems controlled by positive feedback to contain multiple behavioral modes and to have the potential to shift between them when subjected to a continued forcing. Qualitative models of feedback between the tropical forest and the climate describe such a system with two behavioral states: one at high levels of LAI that is resilient and able to recover from even severe stress, and a second mode characterized by runaway behavior that leads to the collapse of the forest and the development of an alternative ecosystem.

A quantitative model based on the parameterization of processes controlling feedbacks confirms the potential for the Amazon forest's ecosystem to experience a major ecological shift in the relatively near future as current deforestation in the Amazon basin caused by logging, agricultural, and mining practices continues. Although the quantitative model is simplistic, the results appear to be robust as model predictions are consistent across a wide range of variables and parameterizations. The results indicate that the point-of-no-return separating resilience and instability may be reached within two to four decades if current rates of deforestation are maintained. A more certain estimate can be obtained if the functions controlling feedbacks are better defined by ongoing research in the Amazon basin. The model also implies that current hopes of creating forest preserves to prevent total loss of the forest and its incredible biodiversity may be misplaced.

Acknowledgments. The author thanks several anonymous reviewers who made suggestions that have improved this paper.

References

Alcock, J., 2001: Systems and graphical analysis of rainforest response to deforestation: A model use of these tools to construct and test knowledge. *Int. J. Environ. Educ. Info.*, **20**, 157–168.

Baidya Roy, S., and R. Avissar, 2002: Impact of land use/land cover change on regional hydrometeorology in Amazonia. *J. Geophys. Res.,* **107**(D20), 8037, doi:10.1029/2000JD000266.

Bazzaz, F. A., 1998: Tropical forests in a future climate: Changes in biological diversity and impact on the global carbon cycle. *Clim. Change,* **39**, 317–336.

Berner, R. A., 1999: A new look at the long term carbon cycle. *GSA Today,* **9**,(11), 1–6.

Bonell, M., 1998: Possible impacts of climate variability and change on tropical forest hydrology. *Clim. Change,* **39**, 215–272.

Brovkin, V., M. Claussen, V. Petoukhov, and A. Ganopolski, 1998: On the stability of the atmosphere–vegetation system in the Sahara/Sahel region. *J. Geophys. Res.,* **103**(D24), 31,613–31,624.

Cochrane, M., 2001: Synergistic interactions between habitat fragmentation and fire in evergreen tropical forests. *Conserv. Biol.,* **15**, 1515–1521.

Cochrane, M., A. Alencar, M. D. Schulze, C. M. Souza Jr., D. C. Nepstad, P. Lefebvre, and E. A. Davidson, 1999: Positive feedbacks in the fire dynamic of closed canopy tropical forests. *Science,* **284**, 1832–1835.

Cox, P. M., R. A. Betts, C. D. Jones, S. A. Spall, and I. J. Totterdell, 2000: Acceleration of global warming due to carbon-cycle feedbacks in a coupled climate model. *Nature,* **408**, 184–187.

Dolman, A. J., M. A. Silva Dias, J. C. Calvet, M. Ashby, A. S. Tahara, C. Delire, P. Kabat, G. A. Fisch, and C. A. Nobre, 1999: Meso-scale effects of tropical deforestation in Amazonia: Preparatory LBA modeling studies. *Ann. Geophys.,* **17**, 1095–1110.

Done, T. J., 1992: Phase shifts in coral reef communities and their ecological significance. *Hydrobiologia,* **247**, 121–132.

Eltahir, E. A. B., and R. L. Bras, 1994: Sensitivity of regional climate to deforestation in the Amazon Basin. *Adv. Water Resour.,* **17**, 101–115.

Eltahir, E. A. B., and J. S. Pal, 1996: Relationships between surface conditions and subsequent rainfall in convective storms. *J. Geophys. Res.,* **101**, 26,237–26,245.

Henderson-Sellers, A., R. E. Dickinson, T. B. Durbridge, P. J. Kennedy, K. McGuffie, and A. J. Pitman, 1993: Tropical deforestation: Modeling local- to regional-scale climate change. *J. Geophys. Res.,* **98**, 7289–7315.

Higgins, P. A. T., M. D. Mastrandrea, and S. H. Schneider, 2002: Dynamics of climate and ecosystem coupling: Abrupt changes and multiple equilibria. *Philos. Trans. R. Soc. London, Ser. B,* **357**, 647–655.

Holling, C. S., 1973: Resilience and stability of ecological systems. *Ann. Rev. Ecol. Syst.,* **4**, 1–23.

Hoare, R., 1998: http://www.worldclimate.com/ (Accessed October 2000).

Jipp, P. H., D. C. Nepstad, D. K. Cassel, and C. Reis de Caravalho, 1998: Deep soil moisture storage and transpiration in forests and pastures of seasonally-dry Amazonia. *Clim. Change,* **39**, 395–412.

Laurance, W. F., S. G. Laurance, L. V. Ferreira, J. M. Rankin-de Merona, C. Gascon, and T. E. Lovejoy, 1997: Biomass collapse in Amazonian forest fragments. *Science,* **278**, 1117–1118.

Lawton, R. O., U. S. Nair, R. A. Pielke Sr., and R. M. Welch, 2001: Climatic impact of tropical lowland deforestation on nearby montane cloud forest. *Science,* **294**, 584–587.

Leopoldo, P. R., W. Franken, and E. Matsui, 1984: Hydrological aspects of the tropical rain forest in the central Amazon. *Interciencia,* **9**, 125–131.

Ludwig, D., D. D. Jones, and C. S. Holling, 1978: Qualitative analysis of insect outbreak systems: the spruce budworm and forest. *J. Animal Ecol.,* **7**, 315–332.

Ludwig, D., B. Walker, and C. S. Holling, 1997: Sustainability, stability, and resilience. *Conserv. Ecol.,* **1**, 1–26.

Marengo, J. A., J. R. Miller, G. L. Russell, C. E. Rosenzweig, and F. Abramopoulos, 1994: Calculations of river-runoff in the GISS GCM: Impact of a new land-surface parameterization and runoff model on the hydrology of the Amazon River. *Clim. Dyn.,* **10**, 349–361.

Mathews, E., 1983: Global vegetation and land use: New high-resolution databases for climate studies. *J. Clim. Appl. Meteorol.*, **22**, 474–487.

Mayle, F. E., R. Burbridge, and T. Killeen, 2000: Millennial-scale dynamics of southern Amazonian rain forests. *Science*, **290**, 2291–2294.

Milsum, J. H., 1968: Mathematical introduction to general system dynamics. *Positive Feedback*, J. H. Milsum, Ed., Pergamon Press, 23–65.

Murakami, S., Y. Tsyboyama, T. Shimizu, M. Fujieda, and S. Noguchi, 2000: Variation of evapotranspiration with stage age and climate in a small Japanese forested catchment. *J. Hydrol.*, **227**, 114–127.

Nepstad, D. C., et al., 1999: Large-scale impoverishment of Amazonian forests by logging and fire. *Nature*, **398**, 505–508.

Nepstad, D., G. Carvalho, A. C. Barros, A. Alencar, J. P. Capobianco, J. Bishop, P. Moutinho, P. Lefebvre, and U. L. Silva Jr., 2001: Road paving, fire regime feedbacks and the future of Amazon forests. *For. Ecol. Manage.*, **5524**, 1–13.

Phillips, O. L., 1997: The changing ecology of tropical forests. *Biodiversity Conser.*, **6**, 291–311.

Salati, E., A. Dall'Olio, E. Matsui, and J. R. Gat, 1979: Recycling water in the Amazon Basin: an isotopic study. *Water Resources Res.*, **15**, 1250–1258.

Salati, E., and P. B. Vose, 1984: Amazon Basin: A system in equilibrium. *Science*, **225**, 129–138.

Santos, P., and A. J. Negri, 1997: A comparison of normalized difference in vegetation index and rainfall for the Amazon and northeastern Brazil. *J. Appl. Meteorol.*, **36**, 958–965.

Scheffer, M., S. H. Hosper, M.-L. Meijer, B. Moss, and E. Jeppesen, 1993: Alternative equilibria in shallow lakes. *Tree*, **8**, 275–279.

Scheffer, M., S. Carpenter, J. A. Foley, C. Folkes, and B. Walker, 2001: Catastrophic shifts in ecosystems. *Nature*, **413**, 591–596.

Shukla, J., C. Nobre, and P. Sellers, 1990: Amazon deforestation and climate change. *Science*, **247**, 1322–1325.

Shuttleworth, W. J., J. H. C. Gash, J. M. Roberts, C. A. Nobre, L. C. B. Molion, and M. de Nazare Goes Ribeiro, 1991: Post-deforestation Amazonian climate: Anglo–Brazilian research to improve prediction. *J. Hydrol.*, **129**, 71–85.

Siegert, F., G. Ruecker, A. Hinrichs, and A. A. Hoffmann, 2001: Increased damage from fires in logged forests during droughts caused by El Niño. *Nature*, **414**, 437–440.

Skole, D., and C. Tucker, 1993: Tropical deforestation and habitat fragmentation in the Amazon: Satellite data from 1978–1988. *Science*, **260**, 1906–1910.

Turner, I. M., and R. T. Corlett, 1996: The conservation value of small, isolated fragments of lowland tropical rain forest. *Tree*, **11**,(8), 331–333.

Wang, G., and E. A. B. Eltahir, 2000: Biosphere–atmosphere interactions over West Africa. II: Multiple climate equilibria. *Q. J. R. Meteorol. Soc.*, **126**, 1261–1280.

Zhang, H., A. Henderson-Sellers, and K. McGuffie, 2001: The compounding effects of tropical deforestation and greenhouse warming on climate. *Clim. Change*, **49**, 309–338.

Earth Interactions is published jointly by the American Meteorological Society, the American Geophysical Union, and the Association of American Geographers. Permission to use figures, tables, and *brief* excerpts from this journal in scientific and education works is hereby granted provided that the source is acknowledged. Any use of material in this journal that is determined to be "fair use" under Section 107 or that satisfies the conditions specified in Section 108 of the U.S. Copyright Law (17 USC, as revised by P.L. 94-553) does not require the publishers' permission. For permission for any other form of copying, contact one of the copublishing societies.